Room Temperature Metastability of Multilayer Graphene Oxide Films

Suenne Kim, Si Zhou, Yike Hu, Muge Acik, Yves J. Chabal, Claire Berger, Walt A. de Heer, Angelo Bongiorno, Elisa Riedo

Room Temperature Metastability of Multilayer Graphene Oxide Films

Suenne Kim[1], Si Zhou[2], Yike Hu[1], Muge Acik[3], Yves J. Chabal[3], Claire Berger [1,4], Walt de Heer [1], Angelo Bongiorno*[2], and Elisa Riedo*[1]

November 29, 2013

[1]*School of Physics, Georgia Institute of Technology, Atlanta, Georgia 30332-0430*

[2]*School of Chemistry & Biochemistry, Georgia Institute of Technology, Atlanta, Georgia 30332-0400*

[3]*Department of Materials Science and Engineering, The University of Texas at Dallas, Richardson, Texas 75080*

[4]*Centre National de la Recherche Scientifique – Institut Néel, Grenoble, B.P. 166, 38042 France*

Graphene oxide has multiple potential applications. The chemistry of graphene oxide and its response to external stimuli such as temperature and light are not well understood and only approximately controlled. This understanding is crucial to enable future applications of this material. Here, a combined experimental and density functional theory study shows that multilayer graphene oxide produced by oxidizing epitaxial graphene via the Hummers method is a metastable material whose structure and chemistry evolve at room temperature with a characteristic relaxation time of about one month. At the quasi-equilibrium, graphene oxide reaches a nearly-stable reduced O/C ratio, and exhibits a structure intensively deprived of epoxide groups and enriched of hydroxyl groups. Our calculations show that the structural and chemical changes are driven by the availability of hydrogen in the oxidized graphitic sheets, which favors the reduction of epoxide groups and the formation of water molecules.

Graphene [1, 2] and graphene-based materials hold great promises for next generation of nanodevices [3–6]. One of the most pressing issues for the technological use of graphene is the possibility to control physical and chemical properties via *ad hoc* functionalization [7]. Thermal, chemical, and optical reduction of graphene oxide have been explored as a route to produce graphene-based materials with the desired electron transport [4, 8–11], mechanical [3], and optical [6] properties. Graphene oxide (GO) in itself is a material of great interest for its potential applications in nano-electronics [4, 8, 12], nano-electromechanical systems [3, 13], sensors [14], polymer composites [15–17], catalysis [18–20], energy storage devices [5, 21, 22], and optics [6]. Graphene does not have a native oxide and harsh chemical treatments are necessary to produce multilayer graphene oxide films [8, 12, 23, 24]. Understanding the chemical transformations occurring in GO in response to external stimuli such as temperature and light remains a challenge [25–29]. Theoretical studies so far have focused primarily on single-layer GO sheets [10, 11, 30, 31], neglecting multilayer GO films.

The traditional route to produce GO films involves several steps: oxidation of graphite via the Hummers method, exfoliation of graphite oxide, dissolution of GO layers in aqueous solution, and deposition of these layers onto a surface from the aqueous dispersion of GO [12, 23]. Here, GO films are obtained by oxidation via the Hummers method of ultra-thin graphene films epitaxially grown on SiC [4, 8]. This method differs from the traditional approach because it does not require the exfoliation/dissolution of the GO layers in aqueous solution and the filtration/deposition on a substrate. A variety of experiments indicate that GO grown by oxidizing graphene films via the Hummers method presents properties equivalent to those of GO obtained by using the traditional approach, with improved film homogeneity and uniformity over extended areas [4, 8] (see Methods and Supplementary Information, Figs. S1-S4).

Here, we report on a combined experimental and density functional theory study of the structural and chemical stability of multilayer GO films. We show that at room temperature multilayer GO is a metastable material undergoing spontaneous chemical modifications and reduction with a relaxation time of $\sim$35 days. The self-limiting processes lead multilayer GO toward a longer-living *quasi*-equilibrium state, in which GO exhibits a structure deprived of epoxide groups and enriched of hydroxyl groups, with a final reduced O/C ratio of 0.38. DFT calculations also show that these structural and chemical changes are driven by the availability of H species in the oxidized graphitic sheets. The excess H species contained in freshly prepared GO films are progressively consumed

via reaction firstly with epoxide groups and secondly with hydroxyl groups to form water molecules which can be realesed. The overall structural and chemical evolution of the metastable GO films is shown to be controlled by diffusion processes.

Multilayer graphene oxide is here synthesized via the Hummers method [32], by oxidation of graphene films grown epitaxially on the C-terminated surface of a SiC wafer [33] (for more details see the Methods part). X-ray photo-emission spectroscopy (XPS) is used to monitor changes of the structural and chemical composition of these GO films with aging time, defined as the time elapsed after oxidation of graphene films. Figure 1a shows a sequence of three C 1s core-level XPS spectra acquired at room temperature from a GO film 1, 40, and 70 days after its synthesis. In between the XPS measurements, the GO films are stored in controlled conditions (T=26$\pm$1°C, dark environment, and relative humidity of 30$\pm$10%). More C 1s spectra acquired from different regions of the same sample and obtained from different GO films are reported in the Supplementary Information (Fig. S3); all curves display the same features and temporal evolution. In particular, they show that the GO films undergo significant chemical changes and spontaneous reduction uniformly across the surface. In this study, C 1s and O 1s core-level spectra are fitted with Gaussian-Lorentzian waveforms after performing a Shirley background subtraction. The C 1s spectra acquired from the GO films are fitted with three peaks. In accordance with previous XPS studies of GO flakes [9, 34], we assign the first peak occurring at $\sim$284.7 eV to C-C, C-H and C vacancies [35]; the second peak at $\sim$286.7 eV is assigned to C-OH (hydroxyl) and C-O-C (epoxide) groups; and the third peak at $\sim$288.3 eV is assigned to C=O (carbonyl) species. The C=O peak in the various C 1s XPS spectra appears to be much smaller than the other two peaks (see Fig. 1a and Supplementary Fig. S3), indicating that carbonyl groups are present in limited number in these GO films. We also remark that differently from previous XPS spectra of GO flakes, the GO films prepared by oxidation of epitaxial graphene do not present carboxyl peaks, indicating that the GO films used in our study lack edges and holes, as also observed in the AFM and optical images reported in the Supplementary Information.

The C 1s XPS spectra of aging GO films show distinctively the increase of the C-C peak, whose area divided by the total C 1s spectral area will be denoted hereafter as P_{G}, and the concurrent decrease of the hydroxyl/epoxide peak, whose area divided by the total C 1s spectral area will be designated as P_{GO}. Figure 1b depicts the $P_{\mathrm{GO}}/P_{\mathrm{G}}$ ratio obtained from XPS spectra of a GO film versus the time elapsed after GO synthesis. The same Figure 1b reports also the time evolution of the oxygen to carbon ratio, P_{oxygen},

in the GO film. P_{oxygen} is estimated from the O 1s/C 1s intensity ratio, corrected by a Scofield relative sensitivity factor of 2.93 (see Supplementary Fig. S4 for the O 1s spectra). Overall, these experimental data indicate that at room temperature GO undergoes significant chemical and structural changes after the sample preparation. The oxygen content and $P_{\mathrm{GO}}/P_{\mathrm{G}}$ ratio decrease with time and stabilize after about 40 and 70 days, respectively. As shown in Fig. 1b, both P_{oxygen} and $P_{\mathrm{GO}}/P_{\mathrm{G}}$ are well-fitted by an exponentially decaying function. The fit parameters show that P_{oxygen} starts out with a value of about 0.44, decays with a time constant of 20 days, and attains a steady state value of 0.38. In the case of $P_{\mathrm{GO}}/P_{\mathrm{G}}$, the corresponding quantities are 1.79, 35 days, and 0.67, respectively. In Fig. 1c, the table reports the values of P_{oxygen} and $P_{\mathrm{GO}}/P_{\mathrm{G}}$ obtained from XPS measurements of three different GO films prepared in similar conditions, at different stages of aging. One of these samples is about a year old. For this aged sample, we obtain values of P_{oxygen} and $P_{\mathrm{GO}}/P_{\mathrm{G}}$ equal to 0.37 and 0.64, in good agreement with the steady state values derived from the fitting analysis of Fig. 1b. This result corroborates the picture that the spontaneous structural and chemical modifications occurring in GO drive this material toward a longer-living quasi-equilibrium state. We remark that kinetics parameters deduced from a recent study [36] of the thermal reduction process of GO flakes in solution cannot explain the here observed spontaneous changes of GO films at room temperature, indicating that we are observing a very distinctive mechanism.

To interpret our experimental results and, at the same time, gain atomistic insight, we have performed DFT calculations. To model multilayer GO, we disregard surface and interface effects, and we use periodic atomistic structures of bulk GO to represent the interior of the GO films. To generate the model structures of bulk GO, we consider an orthorhombic supercell of graphite consisting of 4 graphitic layers and 5×6 graphene unit cells per layer, and including a pseudo-random distribution of O, OH, H, and H_2O species near and between the graphitic layers. The geometry of both the ions and the periodic cell are then optimized via a ∼4-ps long Car-Parrinello molecular dynamics simulation [37]. To relieve the large stress and unfavorable ionic configurations present in the outset structure, the zero-pressure variable-cell molecular dynamics simulations are carried out by damping very gently both electronic and cell degrees of freedom. Similarly to the harsh treatments needed to produce GO films, we use this strategy to generate several realistic model structures of GO at 0 atm and 0 K with a O/C ratio of either 0.44 or 0.38, and a H/C ratio ranging between 0.1 and 0.24. In particular, for a fixed O/C ratio, we generate between 2 and 4 atomistic models including different relative amounts of

epoxide, hydroxyl, chemisorbed hydrogen, and water molecules. The atomistic models include between 370 and 394 atoms.

The model structures of bulk GO generated from DFT exhibit the expected layered structure of an epitaxial film. Interlayer distances depend on both the composition and the amount of water molecules intercalated between the graphitic layers [3]. Due to the large number of chemisorbed species, the graphitic sheets exhibit significant out-of-plane distortions. Notwithstanding, the planar dimensions of the graphitic sheets increase by less than 1% with respect to those of ideal graphene. In addition to epoxide and hydroxyl groups, the model structures show that the oxidized graphene sheets in GO can accommodate both chemisorbed H and, in limited number, carbonyl groups. The atomistic models of GO show that epoxide, hydroxyl, and hydrogen species chemisorbed on the graphitic layers form together with the intercalated H_2O molecules a complex hydrogen bond network (Fig. 2 and Supplementary Fig. S8).

To interpret the XPS measurements, we use DFT to calculate the C 1s XPS spectra of selected model structures of bulk GO. Individual core-level shifts are calculated by carrying out total-energy DFT calculations of the full model structure in which the pseudopotential for the selected C atom is replaced with one that simulates the presence of a screened 1s hole in the core [38, 39]. The computed energy shifts account for the vertical photoexcitation transition and include core-hole relaxation effects [38, 39]. The final spectra are obtained by broadening the individual core-level shifts with a Gaussian function of width 0.5 eV. Absolute binding energies cannot be determined with this approach. Therefore, calculated XPS spectra are compared individually to the experimental ones, and rigidly translated along the energy axis to obtain the best match. Figures 3a and 3b show the experimental XPS spectra of a GO film acquired after an aging time of 1 day and 40 days, respectively, and with a corresponding $P_{oxygen} = 0.44$ (Fig. 3a), and $P_{oxygen} = 0.38$ (Fig. 3b). The same Figures show the calculated XPS spectra (filled circles) obtained from DFT by considering model structures of GO with O/C ratios of 0.44 (Fig. 3a) and 0.38 (Fig. 3b), respectively, and well-defined structural and chemical features (Fig. S8). In particular, the striking agreement between computed and experimental spectra is obtained by considering model structures of GO with a negligible amount of H_2O molecules (1-2% of the total O-content) and carbonyl groups, and a well-defined relative amount of epoxide and hydroxyl species. At fixed C:O:H composition, our DFT calculations indeed show that increasing the amount of intercalated H_2O molecules in multilayer GO leads inevitably to a loss of O species chemisorbed on the graphitic layers

and, regardless of the relative amount of epoxide and hydroxyl groups, to deteriorating the agreement between experiments and theory, confirming the presence of a small amount of intercalated water in the GO films obtained by Hummers oxidation of epitaxial graphene films pre-grown on SiC.

For a more quantitative analysis of our data, we use the experimentally measured values of P_{G}, P_{GO}, and P_{oxygen} to estimate the concentrations of epoxide and hydroxyl groups in multilayer GO. To this end, we assume that, consistently with the DFT results, the amount of intercalated water (or oxygen) molecules in GO is small and hence that the O 1s XPS spectrum results only from epoxide, hydroxyl, and carbonyl groups. By further considering only first next-neighbor effects on C 1s core-level shifts, we can write that:

$$P_{\mathrm{GO}} \cong 2P_{\mathrm{epoxide}} + P_{\mathrm{hydroxyl}} + P_{\mathrm{carbonyl}} \quad (1)$$

$$P_{\mathrm{oxygen}} \cong P_{\mathrm{epoxide}} + P_{\mathrm{hydroxyl}} + P_{\mathrm{carbonyl}}, \quad (2)$$

where P_{epoxide}, P_{hydroxyl}, and P_{carbonyl} are the fractions of epoxide, hydroxyl, and carbonyl groups relative to the total number of carbon atoms in GO. By using P_{G}, P_{GO}, and P_{oxygen} obtained from fitting the experimental XPS spectra, and by taking P_{carbonyl} equal to the ratio of the spectral area of the peak at 288.3 eV (assigned to C=O species) and the total C 1s XPS area, Eqs. (1) and (2) can be solved to estimate P_{epoxide} and P_{hydroxyl}. The results of this analysis for GO films at various stages of aging are shown in Fig. 3c and in the Supplementary Information.

The physical reasonableness of the results and assumptions of the analysis shown in Fig. 3c is corroborated through the use of DFT calculations. Specifically, the model structures of GO yielding optimal agreement with the experiments as shown in Figs. 3a and 3b include fractions (relative to the amount of C) of epoxide, hydroxyl, intercalated water, chemisorbed hydrogen, and carbonyl groups equal to 0.246, 0.179, 0.004, 0.012, and 0.012, respectively, in the case of a film with O/C ratio (i.e. P_{oxygen}) of 0.44, and equal to 0.125, 0.235, 0, 0, and 0.016, respectively, in the case of a O/C ratio of 0.38. These values are in excellent agreement with those obtained from Eqs. (1) and (2) and reported in Fig. 3c. Atomistic models including either a significant amount of intercalated water molecules or different relative number of epoxide and hydroxyl groups worsen considerably the agreement between experimental and DFT spectra. Therefore, although we expect deviations in P_{epoxide} and P_{hydroxyl} obtained from Eqs. (1) and (2) and the experimental XPS spectra due to the uncertainty in the actual content of hydrogen and water in GO,

our study unambiguously shows that multilayer GO films aging at room temperature undergo significant chemical changes. In particular, we find that the fraction of epoxide groups of about 0.23 present in 1-day old films drops to 0.08 in aged (96 days old) films, while the fraction of hydroxyl groups increases from about 0.20 to 0.25. On the basis of DFT calculations, the fraction of water molecules intercalated between the graphitic layers remains at all aging stages negligible, smaller than 3% wt. and 7% wt. in freshly synthesized and aged GO films, respectively.

Infrared spectroscopy measurements (see Supplementary Information, Figs. S5-S6, and Ref. [40]) highlight the presence in GO of C-H species, desorbing at mild temperatures ($\leq$60°C). These species may be at the origin of the room-temperature metastable character of GO. To gain more insight into the room-temperature chemical changes of multilayer GO, we carry out additional DFT calculations (Fig. 4). In particular, we compute the chemisorption energy and diffusion energy barrier of individual H, O, and OH species on a single graphene sheet, as well as the activation energy of the reactions {C-H}+{C-O-C}$\rightarrow${C-OH}+{C-C} and {C-H}+{C-OH}$\rightarrow${C-C}+H_2O, involving species chemisorbed on the graphene sheet and leading to the formation of a physisorbed water molecule. Our DFT calculations show that in presence of chemisorbed H species on graphene, epoxide groups are energetically more costly than hydroxyl groups, which in turn are energetically unfavored with respect to free water (Fig. 4). The DFT calculations also show that both epoxide and hydroxyl groups react readily with the C-H species and that the kinetics of this two-step H-mediated reduction mechanism is controlled entirely by diffusion phenomena. In particular, we find reaction activation energies $\leq$0.15 eV and energy barriers of 0.55 eV, 0.81 eV, and 0.35 eV for the diffusion of a chemisorbed H, epoxide, and hydroxyl groups, respectively. These results indicate that epoxides are the slowest diffusing species and, although at high temperature their diffusion and encounter can lead to the formation of either carbonyl groups or free O_2 [30, 35], at room temperature the reaction of the more rapidly diffusing C-H species with epoxide groups is more likely.

Epoxide rings are strained and more reactive than hydroxyl groups, and the availability of H in freshly synthesized GO films ought to trigger epoxide disruption, strain relief, and the sequential formation of hydroxyl and water species. Our DFT calculations show that these processes may indeed be the mechanisms responsible for the observed structural and chemical changes of GO. According to this picture, the quasi-equilibrium state of GO is attained after consumption of the excess C-H species present in the freshly synthesized films, by means of the following two processes: firstly, reduction of epoxide and hydroxyl

groups and subsequent formation and release of water molecules (within about 40 days as indicated by P_{oxygen} in Fig 1b), and secondly, further reduction of epoxide groups and increase of hydroxyl species (between 40 and 100 days as shown in Fig. 3c).

In summary, in this combined experimental and DFT study we show that multilayer graphene oxide obtained by oxidation via the Hummers method of graphene films grown epitaxially on silicon carbide is structurally and chemically metastable at room temperature. In particular, multilayer GO films undergo spontaneous modifications and reduction with a relaxation time of ∼35 days. These self-limiting processes lead multilayer GO toward a longer-living *quasi*-equilibrium state, in which GO exhibits a structure deprived of epoxide groups, whereas it remains rich in hydroxyl groups, with a final reduced O/C ratio of 0.38. The presence C-H species in GO is found to favor the reduction of epoxides and less extensively hydroxyl groups, and the formation and release of intercalated water molecules. This study provides fundamental understanding of the structural and chemical stability of multilayer graphene oxide. This new understanding will be crucial for the use of this material in industrial applications. Furthermore, this study suggests that a possible route to control structure, chemistry, and properties of GO would be to gauge the hydrogen content in GO, as well as performing the thermal or chemical reduction process after the quasi-equilibrium is attained.

Methods

Sample Preparation.

Graphene films are epitaxially grown on the C-surface of a SiC wafer and the details are reported elsewhere [33]. The Hummers method [32] is employed for the oxidation of the epitaxial graphene films. First, epitaxial graphene on SiC chips are dipped into a $H_2SO_4/NaNO_3$ solution placed in an iced water bath. Second, $KMnO_4$ is added to the solution. The mixture is then transferred to a 35 ^{o}C water bath for about 20 minutes. Deionized (DI) water (23 ml) is added slowly to the mixture. Finally, after 15 minutes, warm DI water (70 ml) and H_2O_2 (1.5 ml) are added to terminate the reaction. The sample is then bought in air, rinsed with DI water, and dried in high purity nitrogen gas. The thickness of the as formed multilayer GO films is deduced by the number of graphene layers present prior to the oxidation process and estimated by ellipsometry experiments. The properties of GO films grown with this procedure are investigated by means of optical imaging, atomic force microscopy, and Raman spectroscopy (see Figs. S1 and S2). Kelvin

probe force microscopy and UHV 4-point transport measurements are used for electrical characterization of the GO films (see Figs. S1 and S2). In general sheet resistances in the range 1-20 GΩ are measured. The data reported here are from three different GO samples, and the number of layers, L, of these samples is as follows: $L = 11$ for the GO film, called GO_A, in Figs. 1a, 1b, 1c, 3, S3a, and S4; $L = N/A$ for GO_B in the table of Fig. 1c, and Supplementary Fig. S3b; and $L = 11$ for GO_C in the table of Fig. 1c, and Supplementary Fig. S3c.

Analytical Measurements.

X-ray Photoelectron Spectroscopy measurements are carried out using a commercial Thermo Scientific K-Alpha XPS system with a focused-beam monochromated Al K-alpha source giving an incident X-ray photon energy of 1486.7 eV. The X-ray spot size is ∼40 μm. We use a 180° double focusing hemispherical analyzer with a 50 eV pass energy. The scans are performed with a step size of 0.1 eV and a dwell time of 50 ms/step. We employ the software XPSPEAK41 for the spectral data analysis. After a Shirley background subtraction and correction for the different X-ray cross-sections using Scofield sensitivity factors, the C 1s spectra are fitted with three Gaussian-Lorentzian peaks with the constrain of equal Gaussian-Lorentzian pre-factors. The three peaks are named in the text as P_{G}, P_{GO}, and P_{carbonyl}. The fits obtained by constraining the full-widths at half-maxima (FWHM) of the three peaks to be equal and the fits obtained by leaving these parameters as free, give results which are the same within the error bar presented in Figs. 1b and 3c, and Table S1. These errors arise from variations in the XPS spectra when acquired from different regions of a given GO sample. We usually acquire XPS spectra from 2 to 5 regions, every single spectrum is shown in Fig. S3. The Doniach-Sunjic asymmetry coefficient is set to zero because the material investigated here, multilayer graphene oxide, is nonmetallic.

Infrared spectroscopy measurements and corresponding results are presented in the Supplementary Information.

Computational methods.

DFT calculations are performed by using the CP code of the QUANTUM-Expresso package [37]. Periodic Γ-point DFT calculations are carried out by using an energy cutoff of 65 Ry for the plane wave basis set, norm-conserving pseudopotentials [41], and a generalized

gradient approximation parametrization for the exchange-correlation energy functional [42]. Variable-cell Car-Parrinello molecular dynamics simulations [37] are carried out to optimize the geometry of the ion positions and cell parameters of periodic structures of GO. Total-energy DFT calculations are performed to calculate C 1 core-level energy shifts [38, 39]. Norm-conserving Troullier-Martins pseudopotentials are generated with the *fhi98PP* package [43]. This computation scheme reproduces excellently the structure, bond energies, and C 1s core-level energy shifts of small H, C, and O containing molecules. Structure and electronic properties of graphene, diamond, and graphite are also reproduced at the expected level of accuracy [44]. Computational strategies for model structure generation and inverse problem solution have been inherited from Refs. [45, 46].

Acknowledgements.

S.K., S.Z., A.B., and E.R. acknowledge the support of the National Science Foundation (CMMI-1100290 and DMR-0820382). Y.H., C.B., and W.H. acknowledge the support of NSF grant DMR-0820382. E.R. acknowledges the support of the NSF grant DMR-0706031 and the Office of Basic Energy Sciences of the U.S. Department of Energy (DE-FG02-06ER46293). Y.J.C. and M.A. acknowledge the support of the Office of Basic Sciences of the U.S. Department of Energy (DE-SC001951). We thank D. Wang, P. Sheehan, and A. R. Laracuente of the U.S. Naval Research Laboratory for the 4-point electrical transport measurements.

Author Contributions

S.K. performed XPS, AFM, and optical experiments. S.Z. carried out DFT calculations. Y.H., C.B., and W.H. synthesized the GO samples. M.A. and Y.C. performed IR measurements. A.B. conceived and designed the theory and analyzed the data. E.R. conceived and designed the experiment and analysized the data. All authors contributed to write the article.

Correspondence.

Correspondence and requests pertaining to experiments and computations should be addressed respectively to E.R. (email: elisa.riedo@physics.gatech.edu) and A.B. (email: angelo.bongiorno@chemistry.gatech.edu).

References

[1] Berger, C. *et al.* Electronic confinement and coherence in patterned epitaxial graphene. *Science* **312**, 1191–1196 (2006).

[2] Geim, A. K. & Novoselov, K. S. The rise of graphene. *Nat. Mater.* **6**, 183–191 (2007).

[3] Medhekar, N. V., Ramasubramaniam, A., Ruoff, R. S. & Shenoy, V. B. Hydrogen bond networks in graphene oxide composite paper: structure and mechanical properties. *ACS Nano* **4**, 2300–2306 (2010).

[4] Wei, Z. *et al.* Nanoscale tunable reduction of graphene oxide for graphene electronics. *Science* **328**, 1373–1376 (2010).

[5] Gao, W. *et al.* Direct laser writing of micro-supercapacitors on hydrated graphite oxide films. *Nature Nanotechnology* **6**, 496–500 (2011).

[6] Loh, K. P., Bao, Q., Eda, G. & Chhowalla, M. Graphene oxide as a chemically tunable platform for optical applications. *Nature Chemistry* **2**, 1015–1024 (2010).

[7] Ruoff, R. S. Graphene: Calling all chemists. *Nature Nanotechnology* **3**, 10–11 (2008).

[8] Wu, X. *et al.* Epitaxial-graphene/graphene-oxide junction: an essential step towards epitaxial graphene electronics. *Phys. Rev. Lett.* **101**, 026801 (2008).

[9] Mattevi, C. *et al.* Evolution of electrical, chemical, and structural properties of transparent and conducting chemically derived graphene thin films. *Adv. Funct. Mat.* **19**, 2577–2583 (2009).

[10] Yan, J.-A., Xian, L. & Chou, M. Y. Structural and electronic properties of oxidized graphene. *Phys. Rev. Lett* **103**, 086802 (2009).

[11] Yan, J.-A. & Chou, M. Y. Oxidation functional groups on graphene: structural and electronic properties. *Phys. Rev. B* **82**, 125403 (2010).

[12] Eda, G., Fanchini, G. & Chhowalla, M. Large-area ultrathin films of reduced graphene oxide as a transparent and flexible electronic material. *Nat. Nanotech.* **3**, 270–274 (2008).

[13] Robinson, J. T. *et al.* Wafer-scale reduced graphene oxide films for nanomechanical devices. *Nano Lett.* **8**, 3441–3445 (2008).

[14] Robinson, J. T., Perkins, F. K., Snow, E. S., Wei, Z. Q. & Sheehan, P. E. Reduced graphene oxide molecular sensors. *Nano Lett.* **8**, 3137–3140 (2008).

[15] Potts, J. R., Dreyer, D. R., Bielawski, C. W. & Ruoff, R. S. Graphene-based polymer nanocomposites. *Polymer* **52**, 5–25 (2011).

[16] Putz, K. W., Compton, O. C., Palmeri, M. J., Nguyen, S. T. & Brinson, L. C. High-nanofiller-content graphene oxide–polymer nanocomposites via vacuum-assisted self-assembly. *Adv. Funct. Mater.* **20**, 3322–3329 (2010).

[17] Dreyer, D. R., Jarvis, K. A., Ferreira, P. J. & Bielawski, C. W. Graphite oxide as a dehydrative polymerization catalyst: a one-step synthesis of carbon-reinforced poly(phenylene methylene) composites. *Macromolecules* **44**, 7659–7667 (2011).

[18] Dreyer, D. R. & Bielawski, C. W. Carbocatalysis: heterogeneous carbons finding utility in synthetic chemistry. *Chem. Sci.* **2**, 1233–1240 (2011).

[19] Dreyer, D. R., Jia, H. & Bielawski, C. W. Graphene oxide: a convenient carbocatalyst for facilitating oxidation and hydration reactions. *Angew. Chem. Int. Ed.* **49**, 6813–6816 (2010).

[20] Jia, H., Dreyer, D. R. & Bielawski, C. W. Graphite oxide as an auto-tandem oxidation–hydration–aldol coupling catalyst. *Adv. Synth. Catal.* **353**, 528–532 (2011).

[21] Wang, D. *et al.* Ternary self-assembly of ordered metal oxide–graphene nanocomposites for electrochemical energy storage. *ACS Nano* **4**, 1587–1595 (2010).

[22] Kim, T. Y. *et al.* High-performance supercapacitors based on poly(ionic liquid)-modified graphene electrodes. *ACS Nano* **5**, 436–442 (2011).

[23] Dikin, D. A. *et al.* Preparation and characterization of graphene oxide paper. *Nature* **448**, 457–460 (2007).

[24] Dreyer, D. R., Ruoff, R. S. & Bielawski, C. W. From conception to realization: an historial account of graphene and some perspectives for its future. *Angew. Chem. Int. Ed.* **49**, 9336–9344 (2010).

[25] Dreyer, D. R., Park, S., Bielawski, C. W. & Ruoff, R. S. The chemistry of graphene oxide. *Chem. Soc. Rev.* **39**, 228–240 (2010).

[26] Gao, W., Alemany, L. B., Ci, L. & Ajayan, P. M. New insights into the structure and reduction of graphite oxide. *Nature Chem.* **1**, 403–408 (2009).

[27] Acik, M. *et al.* The role of intercalated water in multilayered graphene oxide. *ACS Nano* **4**, 5861–5868 (2010).

[28] Rourke, J. P. *et al.* The real graphene oxide revealed: stripping the oxidative debris from the graphene-like sheets. *Angew. Chem. Int. Ed.* **50**, 3173–3177 (2011).

[29] Ekiz, O. Ö., Urel, M., Güner, H., Mizrak, A. K. & Dâna, A. Reversible electrical reduction and oxidation of graphene oxide. *ACS Nano* **5**, 2475–2482 (2011).

[30] Bagri, A. *et al.* Structural evolution during the reduction of chemically derived graphene oxide. *Nature Chem.* **2**, 581–587 (2010).

[31] Wang, L. *et al.* Stability of graphene oxide phases from first-principles calculations. *Phys. Rev. B* **82**, 161406 (2010).

[32] Jr., W. S. H. & Offeman, R. E. Preparation of graphitic oxide. *J. Am. Chem. Soc.* **80**, 1339–1339 (1958).

[33] Berger, C. *et al.* Ultrathin expitaxial graphite: 2d electron gas properties and a route toward graphene-based nanoelectronics. *J. Phys. Chem. B* **108**, 19912–19916 (2004).

[34] Yang, D. *et al.* Chemical analysis of graphene oxide films after heat and chemical treatments by x-ray photoelectron and micro-raman spectroscopy. *Carbon* **47**, 145–152 (2009).

[35] Larciprete, R., Fabris, S., Sun, T., P. Lacovig, A. B. & Lizzit, S. Dual path mechanism in the thermal reduction of graphene oxide. *J. Am. Chem. Soc.* **133**, 17315–17321 (2011).

[36] Jung, I. *et al.* Reduction kinetics of graphene oxide determined by electrical transport measurements and temperature programmed desorption. *J. Phys. Chem. C* **113**, 18480–18486 (2009).

[37] P. Giannozzi *et al.* Quantum espresso: a modular and open-source software project for quantum simulations of materials. *J. Phys.: Condens. Matter* **21**, 395502 (2009).

[38] Pehlke, E. & Scheffler, M. Evidence for site-sensitive screening of core holes at the si and ge(001) surface. *Phys. Rev. Lett.* **71**, 2338–2341 (1993).

[39] Haerle, R., Riedo, E., Pasquarello, A. & Baldereschi, A. sp^2/sp^3 hybridization ratio in amorphous carbon from C 1*s* core-level shifts: X-ray photoelectron spectroscopy and first-principles calculation. *Phys. Rev. B* **65**, 045101 (2001).

[40] Galande, C. *et al.* Quasi molecular fluorescence from graphene oxide. *Sci. Rep.* **1**, 85 (2011).

[41] Troullier, N. & Martins, J. L. Efficient pseudopotentials for plane-wave calculations. *Phys. Rev. B* **43**, 1993–2006 (1991).

[42] Perdew, J. P., Burke, K. & Ernzerhof, M. Generalized gradient approximation made simple. *Phys. Rev. Lett.* **77**, 3865–3868 (1996).

[43] Fuchs, M. & Scheffler, M. Ab initio pseudopotentials for electronic structure calculations of poly-atomic systems using density-functional theory. *Comput. Phys. Commun.* **119**, 67–98 (1999).

[44] Hasegawa, M., Nishidate, K. & Iyetomi, H. Energetics of interlayer binding in graphite: the semiempirical approach revisited. *Phys. Rev. B* **76**, 115424 (2007).

[45] Bongiorno, A. & Pasquarello, A. Oxygen diffusion through the disordered oxide network during silicon oxidation. *Phys. Rev. Lett.* **88**, 125901–125904 (2002).

[46] Bongiorno, A., Pasquarello, A., Hybertsen, M. S. & Feldman, L. C. Transition structure at the Si(100)-SiO_2 interface. *Phys. Rev. Lett.* **90**, 186101 (2003).

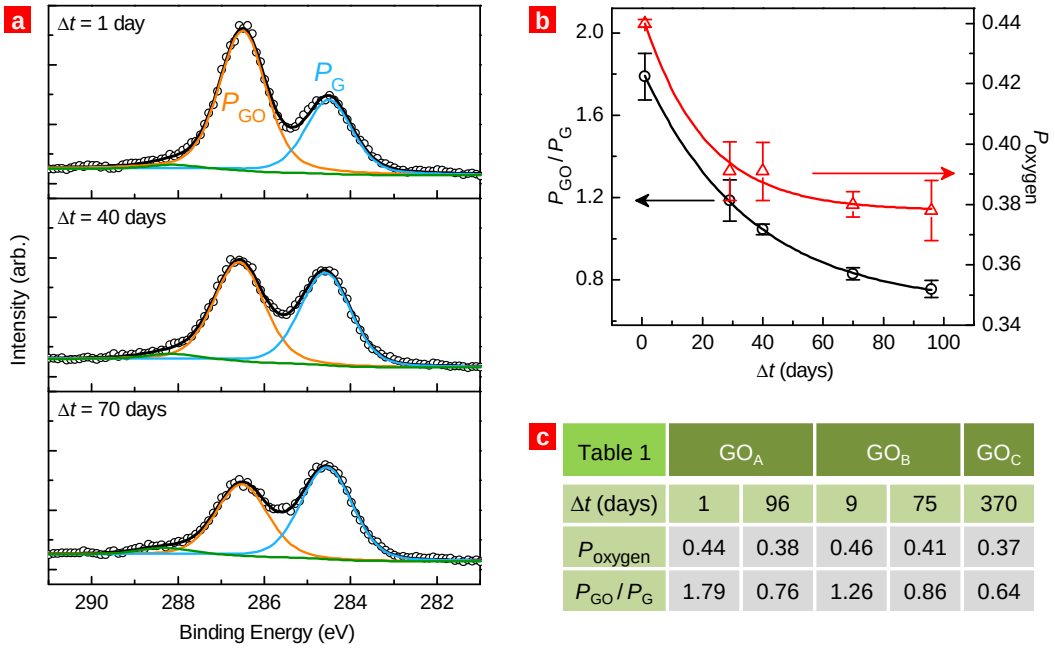

c

Table 1	GO_A		GO_B		GO_C
Δt (days)	1	96	9	75	370
P_{oxygen}	0.44	0.38	0.46	0.41	0.37
P_{GO}/P_G	1.79	0.76	1.26	0.86	0.64

Figure 1: **Room temperature experimental XPS spectra of aged GO films. a**, XPS C 1*s* spectra of a multilayer GO film at increasing aging times at room temperature: 1 (top), 40 (middle), and 70 (bottom) days after GO film synthesis. The spectra are fitted with three Gaussian-Lorentzian peaks. The P_G (blue solid line) peaks is assigned to C-C bonds, and to a small fraction of possible C-H bonds and C vacancies; the P_{GO} peak (orange solid line) is assigned to C species bound in epoxide and hydroxyl groups; the third peak (green solid line) is assigned to carbonyl species. **b**, P_{GO}/P_G in multilayer GO as a function of aging time (black circles), and corresponding oxygen content in the same sample (red triangles). Symbols show experimental values and statistical errors are derived by analyzing XPS spectra acquired from different regions of a given GO sample (see SI). The black and red solid lines show the fits with an exponential decaying function. **c**, Table reporting oxygen content and structural changes with time in three different GO films prepared in similar conditions.

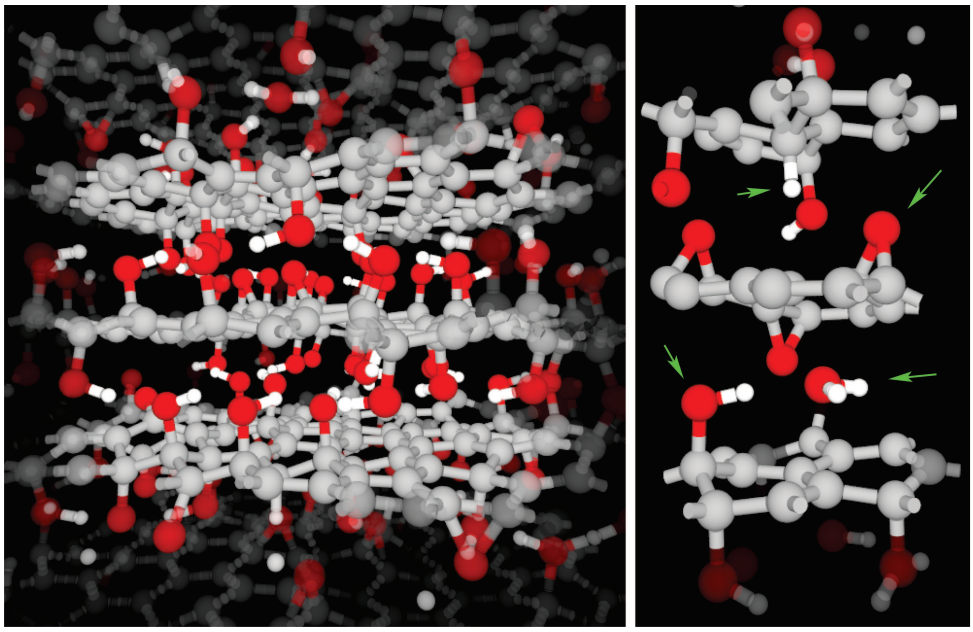

Figure 2: **Atomistic structures of multilayered GO generated from DFT.** Left panel, ball-and-stick illustration of a model structure of GO showing the layered geometry and the complexity of the bonding network on the oxidized carbon basal planes. Right panel, a selected region of the model structure showing the predominant chemical species present in GO films obtained from graphene on SiC; clockwise from top and indicated by the coloured arrows: a hydrogen atom chemisorbed on the basal plane, an epoxide group, an intercalated water molecule, and a hydroxyl species. Gray, red, and white colours are used to represent C, O, and H atoms, respectively. The illustrations show regions of a 390-atom periodic model structure of GO presenting interlayer distances of about 4.22 Å and average intra-layer perpendicular buckling of 0.27 Å.

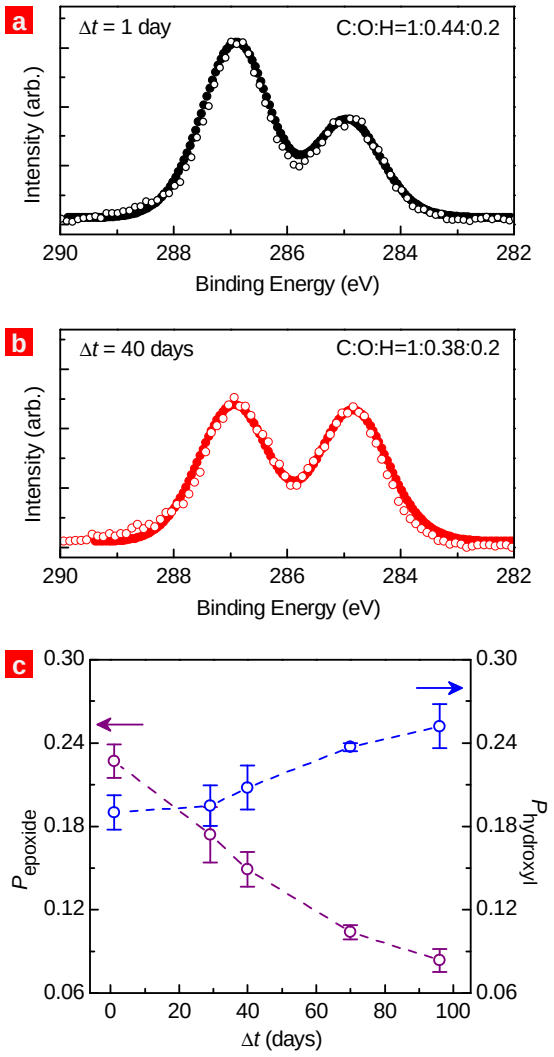

Figure 3: **DFT and experimental XPS spectra. a**, Selected measured and computed C 1*s* XPS spectra of GO. The experimental spectrum is obtained from a freshly synthesized – 1 days old – GO film (black open circles). The theoretical spectrum is extracted from a model structure of GO generated by using DFT simulations (black filled circles). At the outset, composition and structure of the models (indicated in these figures) have been selected on the basis of experimental information. **b**, Selected measured (red open circles) and computed (red filled circles) C 1*s* XPS spectra of GO. The experimental spectrum is obtained from an aged – 40 days old – GO film. **c**, Fraction of epoxide (purple) and hydroxyl (blue) species relative to the amount of C in GO as a function of the aging time at room temperature. These fractions have been derived by obtaining P_{GO}, P_{oxygen}, and P_{carbonyl} from the experimental XPS spectra and by solving the equations (1) and (2). Error bars have been derived by analyzing XPS spectra acquired from different regions of a given GO sample (see SI).

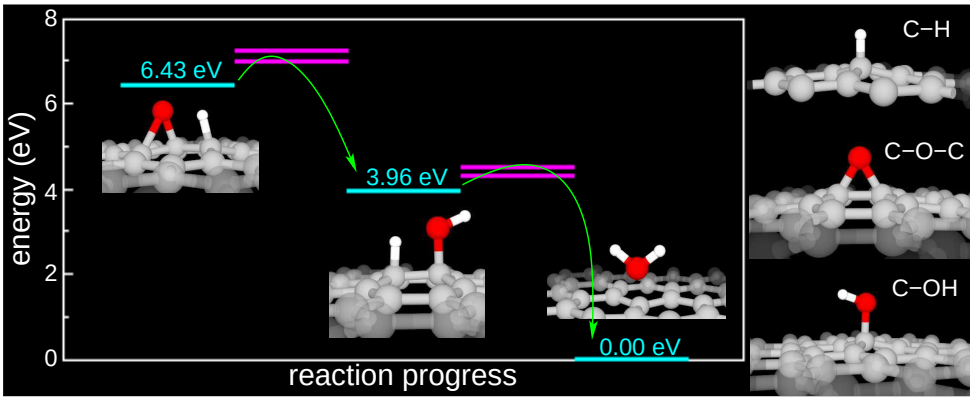

Figure 4: **DFT energy diagram for GO reduction.** Schematic diagram showing the energies involved in the sequential reaction of (left) a H species (C-H) with an epoxide (C-O-C) group to form a hydroxyl (C-OH) species, and (middle) a second C-H species with a C-OH group to form a water molecule physisorbed on the basal plane (right). Reaction transition-state configurations and end-product are shown as insets, and stable configurations of the C-H, C-O-C, and C-OH species on a basal plane are shown on the right of the energy diagram. The cyan-colored segments show the energy of, from left to right, two C-H and one C-O-C, one C-H and one C-OH, and one water molecule physisorbed on graphene; these energies are referred to that of the physisorbed water species. The kinetics of this reduction mechanism is controlled by diffusion processes. Our DFT calculations give activation energies of 0.55 eV, 0.81 eV, and 0.35 eV for the diffusion of a C-H, C-O-C, and C-OH species on the basal plane, respectively. For each reaction step, the magenta-colored segments show the energy of the reacting species when one of them is at the diffusion transition state. C, O, and H atoms are illustrated in gray, red, and white colors, respectively.